

The in-focus variable line spacing plane grating monochromator

R. Reininger

Photon Sciences Directorate, Brookhaven National Laboratory, Upton, NY 11973, United States

ARTICLE INFO

Available online 23 December 2010

Keywords:

Variable-line-spacing grating

Beamline

Soft X-rays

Undulator radiation

ABSTRACT

The in-focus variable line spacing plane grating monochromator is based on only two plane optical elements, a variable line spacing plane grating and a plane pre-mirror that illuminates the grating at the angle of incidence that will focus the required photon energy. A high throughput beamline requires only a third optical element after the exit slit, an aberration corrected elliptical toroid. Since plane elements can be manufactured with the smallest figure errors, this monochromator design can achieve very high resolving power. Furthermore, this optical design can correct the deformations induced by the heat load on the optics along the dispersion plane. This should allow obtaining a resolution of 10 meV at 1 keV with currently achievable figure errors on plane optics. The position of the photon source when an insertion device center is not located at the center of the straight section, a common occurrence in new insertion device beamlines, is investigated.

© 2010 Elsevier B.V. All rights reserved.

1. Introduction

The focusing variable line spacing plane grating monochromator FVLSPGM was proposed by Harada et al. [1] and implemented at a bending magnet beamline at the Photon Factory (PF) [2]. The optical design does not include an entrance slit and it is based on a variable line spacing plane grating and a plane mirror that illuminates the grating such that it focuses a broad energy range at the exit slit. The designed energy resolution of the first FVLSPGM at the PF was not achieved experimentally due to limitations in the monochromator mechanics [2]. A different mechanical design of the FVLSPGM was implemented for the revolver undulator beamline at the PF [3]. With the new mechanical design, the measured resolution was similar to the expected values [3].

The design of the plane mirror mechanism in the SX-700 plane grating monochromator [4], which replaces the translations and rotations of the plane mirror by a rotation around an axis not on the mirror surface, was implemented on a FVLSPGM by Cocco et al. [5] at Elettra. This APPLE-II [6] based undulator beamline was designed for nanospectroscopy requiring the highest possible flux at medium energy resolution. Two APPLE-II based FVLSPGMs using the SX-700 mechanism have been recently implemented, one at the Synchrotron Radiation Center in Wisconsin and one at the Canadian Light Source. The former, described in detail in these proceedings [7], is designed for the energy range 11–270 eV and has only three optical elements to achieve the highest possible transmission. The later, the REIX beamline [8] covering the energy range 80–2000 eV fulfilled its design goals in terms of resolution, flux, and fast polarization switching, and is now open for General User Proposals.

Several other beamlines using the FVLSPGM design and the SX-700 mechanism are at different commissioning [9], procurement [10–13], and design stages [14–16]. Several beamlines are designed to achieve very high resolution at photon energies near 1 keV [10–12,17]. In particular, the DREAMLINE project planned for SSRF [17] is designed to achieve 10 meV at 1 keV, a goal discussed in Section 4.

A different optical concept based on the FVLSPGM and the SX-700 mechanism has successfully been implemented [18] in several beamlines at the SOLEIL synchrotron. The major difference in this optical design is the use of outside diffraction order and positioning the grating upstream of the plane mirror.

2. Focusing with a VLS grating

The line density variation along the length of a variable line spacing (VLS) grating can be expressed as [2]

$$k(w) = k_0(1 + 2b_2w + 3b_3w^2 + 4b_4w^3 \dots) \quad (1)$$

where w is the position on the grating, measured along an axis perpendicular to the grooves, and $w=0$ defines the grating center. The linear coefficient term, b_2 , can be chosen to zero the defocus term in the optical path function:

$$f_{20} = \frac{\cos^2\alpha}{r_1} + \frac{\cos^2\beta}{r_2} - 2b_2nk_0\lambda, \quad (2)$$

at one wavelength, λ , whereas b_3 can be chosen to zero the coma term in the optical path function,

$$f_{30} = \sin\alpha \frac{\cos^2\alpha}{r_1} + \sin\beta \frac{\cos^2\beta}{r_2} - 2b_3nk_0\lambda. \quad (3)$$

In Eqs. (1)–(3), α and β are the incidence and diffraction angles, n is the diffraction order, and r_1 and r_2 are the distances between the

E-mail address: rreinger@bnl.gov

source and the grating and between the grating and the exit slit, respectively. We note in passing that the FVLSPGMs described here do not have an entrance slit.

The optical design of the FVLSPGM includes a plane mirror upstream of the grating that allows to illuminate the grating at the angle of incidence that fulfills simultaneously the grating equation, $nk\lambda = \sin\alpha + \sin\beta$, and the defocus term. This means that in order to operate the monochromator in-focus the c value ($= \cos\beta / \cos\alpha$) is fixed and cannot be changed as in the collimated plane grating monochromator design [19].

One important point of the FVLSPGM optical design is the fact that one can correct for the source position along the dispersion direction by changing the c value. This is being used in the SOLEIL beamlines [18] to compensate for changes in the source position along the dispersion direction since they use two undulators in the straight section. Analytical and ray tracing calculations have also shown that this correction can be used to compensate for the heat load induced deformation on the plane mirror in the monochromator [13].

3. High throughput FVLSPGM

An APPLE II based beamline using a FVLSPGM and covering the energy range 11–270 eV has been commissioned at the Synchrotron Radiation Center (SRC) in Wisconsin and performance results are presented in these proceedings [7]. Since the four straight sections at SRC were already occupied by operating insertion devices (ID), the APPLE II undulator was installed between two bending magnets in a 1 m long section, which allowed for an ID of only 14 periods. To compensate for the lower flux emitted by the device as compared to the 3.5 m undulator serving the over-subscribed plane grating monochromator [20] at SRC, the beamline was designed without an entrance slit and with the minimum number of optical elements: the plane mirror in the monochromator, a VLS grating, and a refocusing mirror. The refocusing element, a horizontally deflecting elliptical toroid, re-images the exit slit in the vertical plane onto the sample position by 2.5:1.4 with the constant sagittal radius of curvature. In the horizontal plane, the undulator source is demagnified by 13.5:1.4 with an elliptical profile along the mirror meridional direction. The elliptical shape eliminates the large coma aberration along the horizontal direction that would have been produced by a constant radius of curvature. A crucial feature of this mirror is the fact that its distance to the slit, rs_1 , and to the sample position, rs_2 , were chosen to minimize the stigmatic coma aberration according to Ref. [21]:

$$rs_2 = \frac{rm_1 rs_1}{2m_1 - rs_1} \quad (4)$$

where m_1 is the distance from the source to the elliptical toroid mirror.

Fig. 1 compares ray tracings using the SHADOW code [22] performed with an astigmatic corrected elliptical toroid (pane a) using the above-mentioned magnifications to an elliptical toroid with larger demagnification of 13.5:0.9 along the horizontal and 2.5:0.9 along the vertical (pane b). Both ray tracings were performed for an energy of 60 eV using the same source and monochromator parameters and an exit slit of 20 μm . As seen in the figures, pane (b) shows a smaller horizontal size but instead of a demagnification along the vertical direction, the vertical size is significantly larger than that of pane (a) being fully dominated by the astigmatic-coma aberration.

We note in passing that an astigmatic-coma-corrected elliptical toroid refocusing mirror such as that described above is used at the REIXS beamline at the Canadian Light Source [8]. The measured

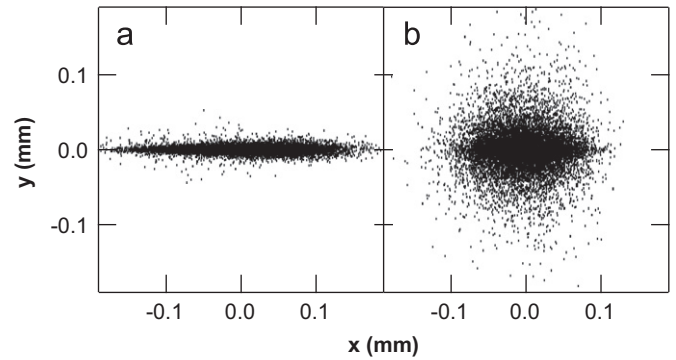


Fig. 1. Ray tracings at the sample plane using (a) the aberration corrected elliptical toroid, (b) with an elliptical toroid designed to obtain a larger horizontal demagnification without including astigmatic coma correction.

spot size is in good agreement with the calculated value and the ray tracings.

4. Achieving 10 meV at 1 keV

In this section we present a FVLSPGM designed to achieve a resolution of 10 meV at 1 keV. This beamline has been designed [17] for the Dreamline project at the Shanghai Synchrotron Radiation Facility (SSRF). The source for this device is a 4.5 m long APPLE II type insertion device. At 1 keV the RMS horizontal source and divergence are 159 μm and 35 μrad , respectively, whereas along the vertical direction the values are 20 μm and 12 μrad . The relevant beamline parameters for the analysis presented here are as follows. A plane mirror located at a distance of 22 m from the source will deflect the beam in the horizontal plane by 1.6°; its main function is to filter the photon energies emitted by the insertion device beyond the range to be used in the beamline. The VLS grating, located at 27 m from the source, disperses in the vertical plane and is preceded by the plane mirror in the monochromator chamber. The exit slit is located at 18 m from the grating. Downstream of the slit, a KB pair focuses the beam at the sample position. We note that the horizontally focusing mirror in the KB pair is the only element focusing along the horizontal direction.

Evidently, the goal of 10 meV at 1 keV requires a high line density grating operated at a relatively large value of c as well as RMS slope errors of $\lesssim 0.1 \mu\text{rad}$ on the plane mirror in the monochromator and on the grating. Such slope errors are currently achievable only on plane surfaces. The sagittal slope error on the horizontally deflecting plane mirror will affect the monochromator resolution. However, the effect of the sagittal slope errors is diminished by the “forgiveness factor”, which in this case is $\sin(0.8^\circ) = 0.014$. Therefore, even for a RMS sagittal slope error of 1 μrad in the first mirror, its effect in the dispersion plane is equivalent to 0.014 μrad .

Fig. 2 shows the resolution due to the source, a 5 μm exit slit, 0.1 μrad RMS slope error on the plane mirror and the grating as well as the vector sum of all contributions. As seen in the figure, the largest contribution over the whole energy range is that of the source. The contribution due to the slope errors on the grating is the second largest and becomes more significant at higher photon energies. From Fig. 2 it is also clear that a resolution of 10 meV at 1 keV is not achieved with this grating and c value. Actually, the resolution contribution from the source size at 1 keV is slightly higher than 10 meV. Increasing the c value to 7 and keeping the same groove density at the grating center (see Fig. 3), lowers the contribution due to the source and the slope errors on the plane mirror by $\approx 4/7$ (approximately since c is not constant). On the

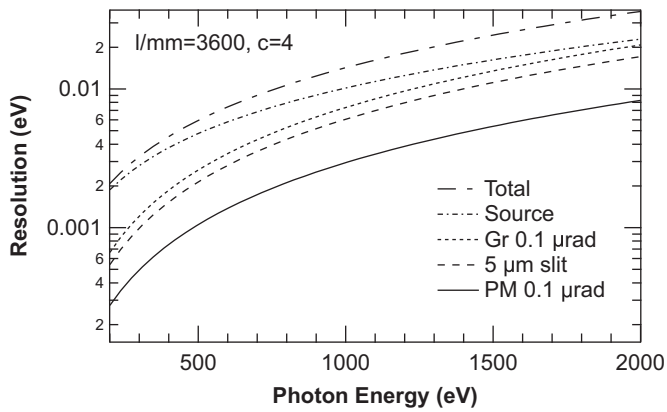


Fig. 2. Resolution due to meridional RMS slope errors of 0.1 μrad on the plane mirror and grating, a 5 μm exit slit, the source, and their vector sum. The grating has 3600 l/mm at its center and is operated with $c=4$.

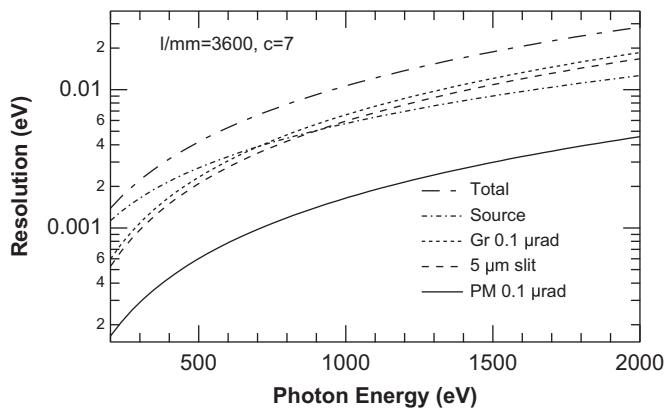


Fig. 3. As Fig. 2, except the gratings operated with $c=7$ instead of $c=4$.

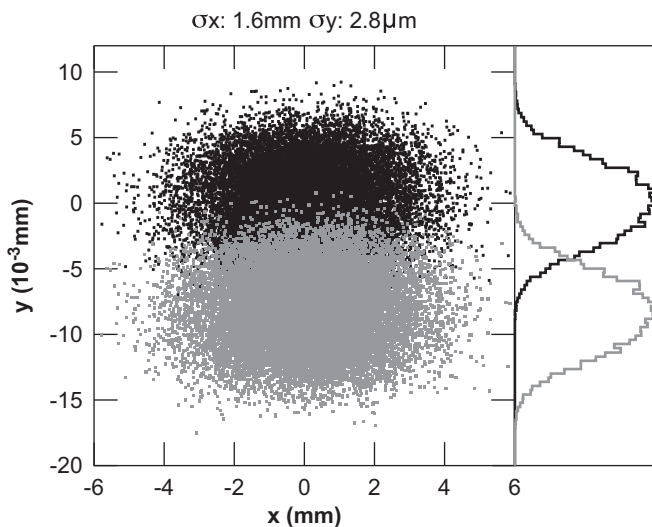


Fig. 4. Ray tracings at the exit plane of the FVLSPGM. Black (gray) dots 1000 eV (1000.01 eV). The grating has 3600 l/mm at its center and is operated with $c=7$. The caption above the figure gives the horizontal and vertical standard deviation sizes.

other hand, the resolution due to the slope errors on the grating and the contribution due to the exit slit are almost unchanged. As seen in Fig. 3, increasing the c value to 7 allows to achieve 10 meV at 1 keV. The ray tracings at the exit slit plane presented in Fig. 4, which include the same slope errors on the optical elements as the

analytical calculations, corroborate the analytical calculations demonstrating that a resolution of 10 meV is achieved with the 3600 l/mm grating and a c value equal to 7.

The collimated plane grating monochromator (CPGM) [19] has achieved excellent resolution and versatility [23] because of its capability of varying the c value and by having the collimating and focusing elements deflecting in the non-dispersion direction, thereby taking advantage of the “forgiveness factor”. The immediate question is whether the CPGM can also achieve a resolution of 10 meV at 1 keV when operating with the same grating and c value that allowed the FVLSPGM to achieve this resolution. To answer this we have ray traced a CPGM using a toroidal mirror instead of the plane mirror in the FVLSPGM and a sagittal cylinder located 1 m downstream of the grating, oriented at a grazing angle of 1.25°. In these calculations we have assumed the same slope errors as before for the plane elements and state-of-the-art RMS sagittal slope errors of 3 μrad on the toroid and the cylinder. The resulting ray tracings shown in Fig. 5 demonstrate that the resolution of 10 meV is not achieved in this case.

Evidently, the use of a high line density grating and a high c value allows to improve the resolution of the monochromator but decreases its optical efficiency, defined as the product of the grating efficiency and the reflectivity of the plane mirror in the monochromator. This is demonstrated in Fig. 6 which shows the optical efficiency of a monochromator equipped with gratings having line

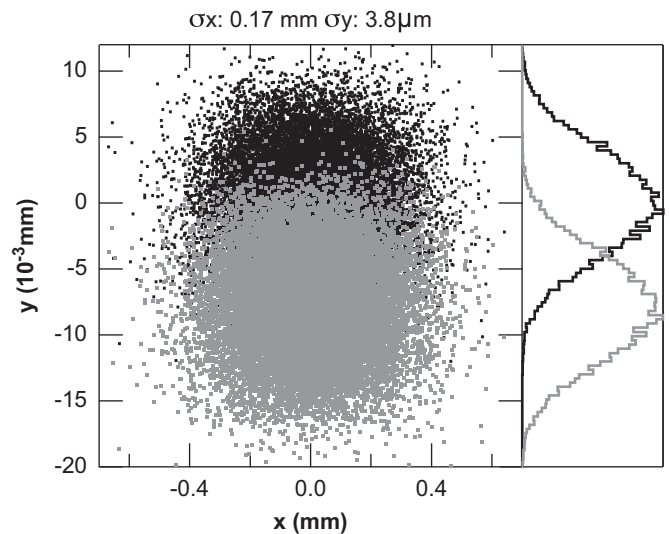


Fig. 5. As Fig. 4 at the exit plane of the CPGM.

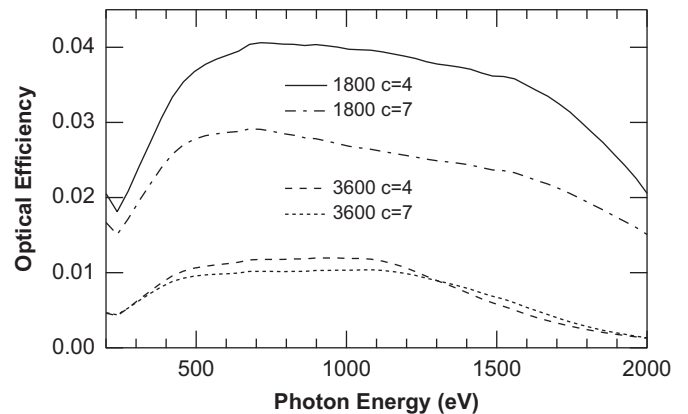


Fig. 6. Optical efficiency of the monochromator (see text) for gratings with line densities of 1800 and 3600 l/mm for two c values.

densities of 1800 and 3600 l/mm when operated with $c=4$ and 7. The grating efficiency was calculated using Neviere's code [24] for blazed gratings and the mirror reflectivity using the Henke tables [25]. As seen in the figure, the optical efficiency with a 3600 l/mm grating operating with $c=7$ is less than 1% in the range covered by the grating and it is smaller by almost a factor of 4 between 200 and 1300 eV as compared to that of a 1800 l/mm grating operating with $c=4$.

Lastly, it is worth mentioning that the stability of the monochromator is essential to achieve a resolving power of 10^5 at 1 keV. The RMS vibrations of the optics in the monochromator need to be at most 0.05 μrad .

5. Source position in canted IDs

One of the CSX beamline [13] branches at the NSLS-II storage ring will achieve fast polarization switching by using two APPLE II insertion devices tuned to different polarizations and a chopper downstream of the exit slit. Two critical requirements were specified for this branch: (i) that both beams have the same photon energy resolution and (ii) that they overlap at the sample position, both requirements within 95% or better. The optical design fulfilling these requirements includes two toroidal mirrors, a FVLSPGM and a cylindrical mirror after the exit slit. The toroids are used to sagittally collimate the beams along the vertical direction and to focus the two beams along the horizontal direction at the same position at the sample. The FVLSPGM focuses the two beams vertically at the exit slit plane, and the meridional cylindrical images the slit at the sample. The 2 m long insertion devices share a straight section and are canted by 0.16 mrad. Since their centers are shifted from the center of the straight section and the electron β functions have their minimum value at the center of the straight section, it is mandatory to determine the position and size of the photon sources to properly design the radii of the two toroids. Actually, this issue is not only relevant for the CSX beamline but also for all the cases where canted undulators are used in the same straight section, which is becoming quite common practice due to the limited number of straight sections in storage rings and the large advantage of an undulator as compared to a bending magnet source. The horizontal and vertical source sizes of the on-axis CSX ID radiation as a function of the distance from the ID centers were calculated at two photon energies using the SRW program [26]. This was accomplished by imaging the source with unity magnification using an ideal lens having a 12.5 m focal length.

Fig. 7 shows the standard deviation of the size (SDS) of the photon beam emitted at 1 keV by a single electron in the undulator as a function of distance from the center of the insertion device. The figure also displays the SDSs obtained after convoluting the single electron emission with the electron beam SDS along the horizontal and vertical directions. The empty (full) circle represent the electron beam vertical (horizontal) SDS at the center of the straight section which, as seen in Fig. 7, is 1.3 m upstream of the center of this insertion device. From the figure one obtains that the waist of the SDS of the single electron emission at 1 keV is 14 μm and it is located at the center of the ID. The waist of the vertical SDS multi-electron emission is ≈ 50 mm towards the center of the ID and its value is 15 μm . The waist of the horizontal SDS is 37 μm and is located 740 mm towards the center of the ID.

When the ID is tuned to emit 200 eV on-axis we obtain that the SDS waist of the single electron emission and the vertical SDS multi-electron is 32 μm and it is located at the center of the insertion ID. The waist of the horizontal SDS at 200 eV is 50 μm and located 250 mm towards the center of the ID.

Based on the results presented above, the sagittal radius of the toroidal mirrors will be designed to collimate the vertical sources

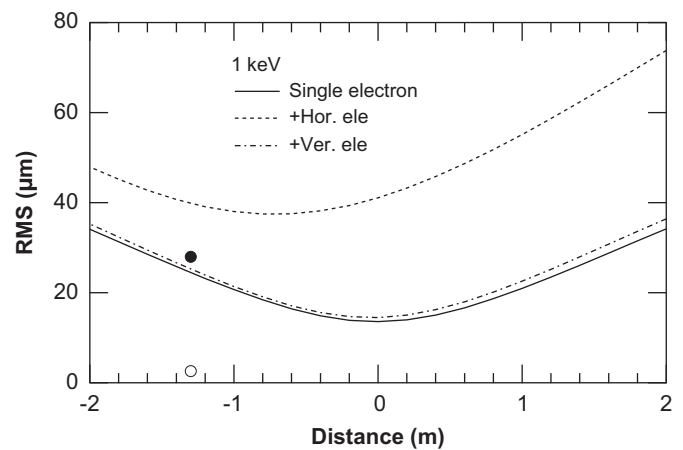


Fig. 7. Solid line: standard deviation of the single electron emission; dash-dotted (dashed): after convolution with the vertical (horizontal) SD of the electron beam size. • (○) represents the electron beam vertical (horizontal) waist at the center of the straight section.

located at the ID centers. The meridional radius of the toroidal mirror focusing the radiation from the upstream (downstream) ID will be designed for a horizontal source located 750 mm downstream (upstream) from the ID center. The latter means that when the IDs are tuned to on-axis photon energies other than 1 keV, the beams will not be at focus at sample, however this is not an issue since the depth of focus is relatively large and both beams will be out of focus almost by the same amount.

6. Conclusion

The principle of the FVLSPGM and two topics related to optical designs using this monochromator were discussed. One is a high throughput undulator based beamline using only three optical elements. The second is a beamline aiming to achieve 10 meV at 1 keV, a goal that seems achievable with today's state-of-the-art plane optical elements. The very high resolution is achieved using a high line density grating and a large c value, choices that significantly lower the beamline transmission.

The vertical source position in undulator based beamlines sharing a straight section is near the center of the undulator whereas the horizontal source position depends on the horizontal electron bunch size and the photon energy. Careful investigation should be done in each case to determine the correct optical setup.

Acknowledgments

I wish to thank O. Tchoubar, C. Sanchez-Hanke, S. Hulbert, and D. Shapiro from BNL and H. Ding from the Institute of Physics, Chinese Academy of Sciences for fruitful discussions. This work was mostly done when working at Scientific Answers & Solutions, 77 Constantine Way, Mount Sinai, NY 11766. Part of it was supported by the U.S. Department of Energy, Office of Science, Office of Basic Energy Sciences, under Contract no. DE-AC02-98CH10886.

References

- [1] T. Harada, M. Itou, T. Kita, Proc. SPIE 503 (1984) 114.
- [2] M. Itou, T. Harada, T. Kita, Appl. Opt. 28 (1989) 146.
- [3] M. Fujisawa, A. Harasawa, A. Agui, M. Watanabe, A. Kakizaki, S. Shin, T. Ishii, T. Kita, T. Harada, Y. Saitoh, S. Suga, Rev. Sci. Instrum. 67 (1996) 345.
- [4] F. Riemer, R. Torge, Nucl. Instr. and Meth. 208 (1983) 313.
- [5] D. Cocco, M. Marsi, M. Kiskinova, K. Prince, T. Schmidt, S. Heun, E. Bauer, Proc. SPIE 3767 (1999) 271.

- [6] S. Sasaki, Nucl. Instr. and Meth. A 347 (1994) 83.
- [7] M. Severson, M. Bissen, M. Fisher, G. Rogers, R. Reininger, M. Green, D. Eisert, B. Tredinnick, Nucl. Instr. and Meth. A, this issue, doi:10.1016/j.nima.2010.12.029.
- [8] REIXS beamline at the CLS <http://exshare.lightsource.ca/REIXS/Pages/default.aspx>.
- [9] R. Reininger, A.R.B. de Castro, Nucl. Instr. and Meth. A 538 (1–3) (2005) 760.
- [10] IEX beamline at APS, see <http://journals.iucr.org/s/issues/2009/06/00/s090600aps.pdf>.
- [11] ID08 at the ESRF, see http://www.esrf.eu/UsersAndScience/Experiments/ElectStructMagn/beamline-portfolio/CDR_UPBL07_future-ID08.pdf.
- [12] P04 at PETRA III, see http://petra3.desy.de/beamlines/beamlines/beamlines/xuv_beamline/index_eng.html.
- [13] R. Reininger, K. Kriesel, S.L. Hulbert, C. Sánchez-Hanke, D.A. Arena, Rev. Sci. Instrum. 79 (2008) 033108;
R. Reininger, C. Sanchez-Hanke, S.L. Hulbert, in: AIP Conference Proceedings, vol. 1234, 2010, p. 383.
- [14] QMSC beamline at the CLS, personal communication.
- [15] R. Reininger, J. Woicik, S. Hulbert, D. Fischer, Nucl. Instr. and Meth. A, this issue, doi: 10.1016/j.nima.2010.11.172.
- [16] MAESTRO at ALS, see https://sng-web.als.lbl.gov/groups/maestro/wiki/a7c16/MAESTRO_Future.html.
- [17] R. Reininger, R. Tai, Y. Hu, Y. Wang, F. Guo, H. Ding, in preparation.
- [18] F. Polack, B. Lagarde, M. Idir, in: AIP Conference Proceedings, vol. 879, 2007, p. 655.
- [19] R. Follath, F. Senf, Nucl. Instr. and Meth. A 390 (1997) 388.
- [20] R. Reininger, S. Crossley, M. Lagergren, M. Severson, R. Hansen, Nucl. Instr. and Meth. A 347 (1994) 304.
- [21] M. Chrisp, Appl. Opt. 22 (1983) 1508.
- [22] C. Welna, G. Chen, F. Cerrina, Nucl. Instr. and Meth. A 347 (1994) 344.
- [23] R. Follath, Nucl. Instr. and Meth. A 467–468 (2001) 418.
- [24] M. Neviere, P. Vincent, R. Petit, Nouv. Rev. Opt. 5 (1974) 65.
- [25] B. Henke, E. Gullikson, J. Davis, At. Data Nucl. Data Tables 54 (1993) 181.
- [26] O. Chubar, P. Elleaume, in: Proceedings of EPAC'98, 6th European Particle Accelerator Conference, 1998, p. 1177.